Wireless Pers Commun (2015) 81:1143–1157
DOI 10.1007/s11277-014-2176-2

BER Analysis for BPSK Based SIM–FSO Communication System Over Strong Atmospheric Turbulence with Spatial Diversity and Pointing Errors

K. Prabu · D. Sriram Kumar

Published online: 13 November 2014

Abstract Free space optical communication (FSO) has much attention in recent years for the applications viz. inter-satellite, deep space communications, inter and intra chip communications. The performance of FSO systems sternly suffers from atmospheric turbulence due to the random nature of weather conditions. Spatial diversity is an emerging technique for improving the performance of the system over strong atmospheric turbulences. In this paper, the error rate performance of binary phase shift keying based subcarrier intensity modulated free space optical (SIM–FSO) communication system over gamma–gamma channel with pointing errors is investigated. Novel closed-form analytical expressions are derived for the average bit error rate of single-input multiple-output FSO (SIMO–FSO) system with various combining schemes. The error rate performance of SISO and SIMO–FSO systems are compared in terms of 2D and 3D plots.

Keywords Free space optics · Pointing errors · Strong atmospheric turbulence · Bit error rate · Single-input multiple-output

1 Introduction

Free space optical (FSO) communication provides high data rate and secure communication with low maintenance cost and less deployment time [1]. FSO is the best complement technology to radio frequency (RF) communication, due to huge capacity and greater bandwidth, superior protection against interference, lesser power consumption and compact transceiver architecture [2]. The performance of the FSO systems purely depends on the external atmospheric conditions caused by the variations of the refractive index. Various channel

K. Prabu (✉) · D. S. Kumar
Department of Electronics and Communication Engineering, National Institute of Technology (NIT), Tiruchirappalli 620015, India
e-mail: nitprabu@gmail.com

D. S. Kumar
e-mail: srk@nitt.edu

models are developed to evaluate the impact of atmospheric turbulence such as, log-normal, negative exponential and gamma–gamma model [3,4]. The log-normal distribution is valid only in weak turbulence and the gamma–gamma distribution is found to be the most suitable for moderate to strong turbulence channels [5]. The strong atmospheric channel model with the mutual effect of atmospheric turbulence and pointing error effects are investigated in [6–8]. The wireless optical link impaired by absorption, scattering, diffraction and atmospheric turbulence. The random variations in the refractive index of atmosphere cause random fluctuations in both amplitude and phase of the transmitting optical beam which result in fading, beam spread, and angular spread [9]. As per previous studies, the various solutions to mitigate the effects of atmospheric turbulence are error control coding in conjunction with interleaving, maximum likelihood sequence detection and spatial diversity [10,11].

The different modulation formats used in FSO systems are on-off keying (OOK), binary phase shift keying (BPSK) [4], pulse position modulation (PPM) [12], differential phase shift keying (DPSK) [13], polarization shift keying (PolSK) [14] and subcarrier intensity modulation (SIM) [3,4]. The OOK is the simplest and widely used modulation format in FSO systems. But, it requires an adaptive threshold to perform optimally and very sensitive to atmospheric turbulence [3]. The drawbacks of OOK modulation are overcome by PPM; however it requires complex transceiver design and suffers from poor bandwidth efficiency. The modulation scheme plays a vital role to decide the power efficiency in FSO systems. The phase angular modulation formats, such as BPSK and DPSK are highly sensitive to the phase noise effects [15]. PolSK bids greater immunity to the phase noise and the atmospheric turbulence. The SIM was first proposed in the optical wireless communications (OWC) application in [16] and then it is employed with various phase-shift keying (PSK) modulations over different atmospheric turbulence channels. Recently, the performances of FSO systems are analyzed including the combined effect of atmospheric turbulence and misalignment fading over strong atmospheric channels [6,7]. A multiple-input multiple-output FSO (MIMO–FSO) system improves the bit error rate (BER) performance over strong atmospheric turbulence channels [17]. Single-input multiple-output FSO (SIMO–FSO) systems with diversity techniques can offer signal redundancy which mitigates the fading effects and significantly improve the transmission rate [18]. In [19], the outage probability of MIMO–FSO system is investigated.

The tradeoff between BER and link distance by compensating the phase noise using OFDM pilot subcarriers in Coherent Optical OFDM Systems is studied in [20]. A very high bitrate is achieved through an all-optical fiber distributed indoor system providing wireless cells in [21]. The availability for FSO and MMW systems for the region of Uruguay (South America) is studied in [22]. In [23], the performance of wireless underwater communications for different ocean water types is analyzed.

In a recent work, [24], SIM based DPSK scheme in FSO system is considered and its BER performance is evaluated over MIMO–FSO links which follow the gamma–gamma distribution. The performance analysis of multi-beam FSO system employed in the diversity or multiplexing scheme is studied in [18]. In this paper, the BER performance of BPSK based SIM–FSO system over gamma–gamma distributed strong atmospheric channel with pointing error is investigated. The novel closed form BER expressions are derived for FSO links with multiple apertures at the receiver.

The rest of the paper is organized as follows: Sect. 2 discusses the system and channel model used. In Sect. 3 and 4, the average BER for SISO and SIMO are discussed. Section 5 describes the numerical results with graphical analysis. Finally, concluding remarks are highlighted in Sect. 6.

2 System and Channel model

2.1 System Model

An FSO communication system with M transmission apertures and N reception apertures over a discrete time ergodic channel with additive white Gaussian noise (AWGN) is considered. The binary input data are modulated by using BPSK–SIM and transmitted through the telescope into strong atmospheric turbulence. The received electrical signal at the n^{th} receiver aperture is given by [25]

$$r_n = x\gamma \sum_{m=1}^{M} h_{mn} + v_n, \quad n = 1, 2, \ldots..N \tag{1}$$

where x is the transmitted signal, γ is the detector responsivity, h_{mn} is the irradiance from the m^{th} transmitter and n^{th} receiver, v_n is the AWGN with zero mean and variance $\sigma_v = N_0/2$. The irradiance $'h_{mn}'$ models the optical intensity fluctuations resulting from atmospheric loss, turbulence and fading is given as [6]

$$h_{mn} = h_{l_{mn}} h_{s_{mn}} h_{p_{mn}} \tag{2}$$

where $h_{l_{mn}}$ is the attenuation due to beam extinction and path loss from the m^{th} transmitter and n^{th} receiver, $h_{s_{mn}}$ due to scintillation effects and $h_{p_{mn}}$ due to the geometric spread and pointing errors.

2.2 Channel Model

The atmospheric path loss is modeled by Beers-Lambert law is given as [26]

$$h_{l_{mn}} = e^{-\sigma L_{mn}} \tag{3}$$

where σ is the attenuation coefficient and L_{mn} is the propagation distance of m^{th} transmitter and the n^{th} receiver.

The strong atmospheric turbulence can be modeled by gamma–gamma distribution with scintillation parameters α and β, which are indicated as functions of the Rytov variance and a geometry factor. The probability density function (PDF) of the gamma–gamma distribution is given by [26]

$$f_{h_{s_{mn}}}\left(h_{s_{mn}}\right) = \frac{2(\alpha_{mn}\beta_{mn})^{(\alpha_{mn}+\beta_{mn})/2}}{\Gamma(\alpha_{mn})\Gamma(\beta_{mn})} h_{s_{i,j}}^{(\alpha+\beta)/2-1} K_{(\alpha_{mn}-\beta_{mn})}\left(2\sqrt{\alpha_{mn}\beta_{mn}h_{s_{i,j}}}\right) \tag{4}$$

where α and β are the effective number of large and small scale turbulent eddies, $\Gamma(\cdot)$ is the gamma function and $K_{(\alpha-\beta)}$ is the modified Bessel function of the second kind of order $(\alpha - \beta)$.

The signal fading due to pointing errors can be defined based on a circular detection aperture of radius r and a Gaussian beam. The PDF of h_p is given by [6]

$$f_{h_p}\left(h_p\right) = \frac{\xi_{mn}^2}{A_0^{\xi_{mn}^2}} h_p^{\xi_{mn}^2-1}, 0 \le h_p \le A_0 \tag{5}$$

where $A_0 = [erf\,(v)]^2$ is the fraction of the collected power at $r = 0$. The Gauss error function $erf\,(\cdot)$ is defined as $erf\,(x) = \frac{2}{\sqrt{\pi}} \int_0^x e^{-t^2} dt$. The radial distance is denoted as r

and ξ is the ratio between the equivalent beam radius at the receiver and the pointing error displacement (jitter) standard deviation at the receiver.

The combined channel distribution for strong atmospheric turbulence regime is given by [27]

$$f_{h_{i,j}}\left(h_{i,j}\right) = \frac{2\xi_{mn}^2(\alpha_{mn}\beta_{mn})^{(\alpha_{mn}+\beta_{mn})/2}}{\left(A_0 h_{l_{i,j}}\right)^{\xi_{mn}^2}\Gamma(\alpha_{mn})\Gamma(\beta_{mn})} h_{i,j}^{\xi_{mn}^2-1} \times \int_{h_{i,j}/A_0 h_{l_{i,j}}}^{\infty} h_{s_{i,j}}^{(\alpha_{mn}+\beta_{mn})/2-1-\xi_{mn}^2} K_{(\alpha_{mn}-\beta_{mn})}\left(2\sqrt{\alpha_{mn}\beta_{mn}h_{s_{i,j}}}\right) dh_{s_{i,j}} \quad (6)$$

where α and β are the effective number of large and small scale turbulent eddies, $\Gamma(\cdot)$ is the gamma function, $K_{(\alpha-\beta)}$ is the modified Bessel function of the second kind of order $(\alpha-\beta)$. The effective number of large and small scale turbulent eddies α and β for a spherical wave are given by [27],

$$\alpha = \left[exp\left(\frac{0.49\delta_n^2}{\left(1+0.18d^2+0.56\delta_n^{12/15}\right)^{7/6}} \right) - 1 \right]^{-1} \quad (7)$$

$$\beta = \left[exp\left(\frac{0.51\delta_n^2\left(1+0.69\delta_n^{12/15}\right)^{-5/6}}{\left(1+0.9d^2+0.62d^2\delta_n^{12/15}\right)^{5/6}} \right) - 1 \right]^{-1} \quad (8)$$

where $d = \sqrt{kD^2/4L}$, $k = 2\pi/\lambda$, is the optical wave number, with λ being the operational, L is the length of the optical link and D is the receiver's aperture diameter. The parameter δ_n^2 is the Rytov variance and is given as, $\delta_n^2 = 0.5C_n^2k^{7/6}L^{11/6}$ and the C_n^2 represents the refractive index structure parameter.

The strong atmospheric turbulence is modeled using gamma–gamma distribution channel with pointing errors. The probability density function (PDF) of the considered channel model is given by using the Meijer G function [28]

$$f_{h_{mn}}\left(h_{mn}\right) = \frac{\alpha_{mn}\beta_{mn}\xi_{mn}^2}{A_{0_{mn}}h_{l_{mn}}\Gamma(\alpha_{mn})\Gamma(\beta_{mn})} G_{1,3}^{3,0}\left[\frac{\alpha_{mn}\beta_{mn}h_{mn}}{A_{0_{mn}}h_{l_{mn}}} \middle| \begin{matrix} \xi_{mn}^2 \\ -1+\xi_{mn}^2, \alpha_{mn}-1, \beta_{mn}-1 \end{matrix} \right] \quad (9)$$

where α_{mn} and β_{mn} represent the effective number of large and small scale turbulent eddies, $\Gamma(\cdot)$ is the gamma function.

3 Average BER for SISO–FSO Links

For a coherent BPSK based SIM–FSO communication system, the probability of conditional BER depending on the intensity fluctuation [4] can be expressed as

$$P_{ec,SISO}\left(h\right) = Q\left(\frac{h\gamma}{\sqrt{2}\sigma_n}\right) = 0.5 \times \text{erfc}\left(\frac{h\gamma}{2\sigma_n}\right) \quad (10)$$

where γ is the photo detector responsivity, σ_n^2 is the variance of the channel noise and $Q\left(\cdot\right)$ is the Gaussian Q function related to the complementary error function $\text{erfc}\left(\cdot\right)$ as $2Q\left(\sqrt{2}x\right) = \text{erfc}\left(x\right)$.

For a strong atmospheric turbulence channel with gamma–gamma distribution, the average BER P_e, can be obtained by averaging Eq. (10) over the PDF of h can be computed as

$$P_{e,SISO} = \int_0^\infty P_{ec,SISO}\,(h)\; f_h\,(h)\, dh \tag{11}$$

By using Eqs. (9) and (10) in (11), the average BER can be obtained as

$$P_{e,SISO} = \frac{\alpha\beta\xi^2}{A_0 h_l \Gamma(\alpha)\Gamma(\beta)} \times \int_0^\infty 0.5\,\mathrm{erfc}\left(\frac{h\gamma}{2\sigma_n}\right) \times G_{1,3}^{3,0}\left[\frac{\alpha\beta h}{A_0 h_l}\middle|_{-1+\xi^2,\alpha-1,\beta-1}^{\xi^2}\right] dh \tag{12}$$

By expressing the erfc(·) as Meijer G function [29, Eq. (8.4.14.2)], the average BER of BPSK–SIM [30] can be expressed in a closed-form by utilizing [31, Eq. (21)]. The proof is available in Appendix 1.

$$P_{e,SISO} = \frac{2^{\alpha+\beta-4}\xi^2}{\sqrt{\pi^3}\Gamma(\alpha)\Gamma(\beta)} G_{7,4}^{2,6}\left[\frac{4\gamma^2 A_0^2 h_l^2}{\sigma_n^2\alpha^2\beta^2}\middle|_{0,\frac{1}{2},\frac{-\xi^2}{2},\frac{-\xi^2+1}{2}}^{\frac{1-\xi^2}{2},\frac{2-\xi^2}{2},\frac{1-\alpha}{2},\frac{2-\alpha}{2},\frac{1-\beta}{2},\frac{2-\beta}{2},1}\right] \tag{13}$$

The above average BER expression is expressed in terms of average SNR can be expressed as

$$P_{e,SISO} = \frac{2^{\alpha+\beta-4}\xi^2}{\sqrt{\pi^3}\Gamma(\alpha)\Gamma(\beta)} G_{7,4}^{2,6}\left[\frac{8SNR\cdot \mathrm{A}_0^2}{\alpha^2\beta^2}\middle|_{0,\frac{1}{2},\frac{-\xi^2}{2},\frac{-\xi^2+1}{2}}^{\frac{1-\xi^2}{2},\frac{2-\xi^2}{2},\frac{1-\alpha}{2},\frac{2-\alpha}{2},\frac{1-\beta}{2},\frac{2-\beta}{2},1}\right] \tag{14}$$

4 Average BER for SIMO–FSO Links

The primary solution for a strong atmospheric turbulence channel is spatial diversity technique, which can be applied either at the transmitter (MISO) or at the receiver (SIMO) or at both the sides (MIMO). The average BER for MIMO–FSO links can be calculated from [25]

$$P_{e,MIMO} = \int_0^\infty f_{\boldsymbol{h}}\,(\boldsymbol{h})\; Q\left(\frac{\gamma}{MN\sqrt{2}\sigma_n}\sqrt{\sum_{n=1}^{N}\left(\sum_{m=1}^{M} h_{mn}\right)^2}\right) d\boldsymbol{h} \tag{15}$$

where $f_{\boldsymbol{h}}\,(\boldsymbol{h})$ is the joint PDF of vector $\boldsymbol{h} = (h_{11}, h_{12}, \ldots h_{MN})$ of length MN.

To improve the BER performance in strong atmospheric turbulence, multiple receiver apertures that are added at the receiver mitigate the turbulence induced irradiance fluctuation. Introducing diversity in the receiver is known as SIMO. The various diversity techniques used in the receiver are, optimal combining (OC), equal gain combining (EGC) and selection combining (SC).

4.1 Optimal Combining

The electrical SNR of the FSO system with OC can be described as

$$SNR_{OC} = \frac{\gamma^2}{2N\sigma_n^2}\sum_{n=1}^{N} h_n^2 \tag{16}$$

The conditional BER of the system can be computed as

$$P_{ec,OC}(\boldsymbol{h}) = Q\left(\sqrt{SNR_{OC}}\right) = Q\left(\frac{\gamma}{\sqrt{2N}\sigma_n}\sqrt{\sum\nolimits_{n=1}^{N} h_n^2}\right) \tag{17}$$

The OC diversity is applied at the receiver, then the average BER of SIMO–FSO is written as

$$P_{e,OC} = \int_0^\infty Q\left(\frac{\gamma}{\sqrt{2N}\sigma_n}\sqrt{\sum\nolimits_{n=1}^{N} h_n^2}\right) f_{\boldsymbol{h}}(\boldsymbol{h})\, d\boldsymbol{h} \tag{18}$$

The integral in Eq. (18) is simplified by using the approximation of Q-function [32, Eq. (14)] to obtain the average BER as

$$P_{e,OC} \approx \frac{1}{12}\prod_{n=1}^{N}\int_0^\infty f_{h_n}(h_n)\, e^{-\left(\frac{\gamma^2 h_n^2}{4N\sigma_n^2}\right)} dh_n + \frac{1}{4}\prod_{n=1}^{N}\int_0^\infty f_{h_n}(h_n)\, e^{-\left(\frac{\gamma^2 h_n^2}{3N\sigma_n^2}\right)} dh_n \tag{19}$$

By applying Eq. (9) in (19) and express the exp(·) as Meijer G function [31, Eq. (11)], the average BER of BPSK–SIM [30] can be evaluated using [31, Eq. (21)] as

$$\begin{aligned} P_{e,OC} \approx{}& \frac{1}{12}\prod_{n=1}^{N}\frac{2^{\alpha_n+\beta_n-3}\xi_n^2}{\pi\Gamma(\alpha_n)\Gamma(\beta_n)} G_{6,3}^{1,6}\left[\frac{4\gamma^2 A_0^2 h_l^2}{N\sigma_n^2\alpha_n^2\beta_n^2}\middle|\begin{matrix}\frac{1-\xi_n^2}{2}, \frac{2-\xi_n^2}{2}, \frac{1-\alpha_n}{2}, \frac{2-\alpha_n}{2}, \frac{1-\beta_n}{2}, \frac{2-\beta_n}{2} \\ 0, \frac{-\xi_n^2}{2}, \frac{1-\xi_n^2}{2}\end{matrix}\right] \\ &+ \frac{1}{4}\prod_{n=1}^{N}\frac{2^{\alpha_n+\beta_n-3}\xi_n^2}{\pi\Gamma(\alpha_n)\Gamma(\beta_n)} G_{6,3}^{1,6}\left[\frac{16\gamma^2 A_0^2 h_l^2}{3N\sigma_n^2\alpha_n^2\beta_n^2}\middle|\begin{matrix}\frac{1-\xi_n^2}{2}, \frac{2-\xi_n^2}{2}, \frac{1-\alpha_n}{2}, \frac{2-\alpha_n}{2}, \frac{1-\beta_n}{2}, \frac{2-\beta_n}{2} \\ 0, \frac{-\xi_n^2}{2}, \frac{1-\xi_n^2}{2}\end{matrix}\right] \end{aligned} \tag{20}$$

The proof is available in Appendix 2.

In terms average SNR, the Eq. (20) can be rewritten as

$$\begin{aligned} P_{e,OC} \approx{}& \frac{1}{12}\prod_{n=1}^{N}\frac{2^{\alpha_n+\beta_n-3}\xi_n^2}{\pi\Gamma(\alpha_n)\Gamma(\beta_n)} G_{6,3}^{1,6}\left[\frac{8SNR\cdot A_0^2}{N\alpha_n^2\beta_n^2}\middle|\begin{matrix}\frac{1-\xi_n^2}{2}, \frac{2-\xi_n^2}{2}, \frac{1-\alpha_n}{2}, \frac{2-\alpha_n}{2}, \frac{1-\beta_n}{2}, \frac{2-\beta_n}{2} \\ 0, \frac{-\xi_n^2}{2}, \frac{1-\xi_n^2}{2}\end{matrix}\right] \\ &+ \frac{1}{4}\prod_{n=1}^{N}\frac{2^{\alpha_n+\beta_n-3}\xi_n^2}{\pi\Gamma(\alpha_n)\Gamma(\beta_n)} G_{6,3}^{1,6}\left[\frac{32SNR\cdot A_0^2}{3N\alpha_n^2\beta_n^2}\middle|\begin{matrix}\frac{1-\xi_n^2}{2}, \frac{2-\xi_n^2}{2}, \frac{1-\alpha_n}{2}, \frac{2-\alpha_n}{2}, \frac{1-\beta_n}{2}, \frac{2-\beta_n}{2} \\ 0, \frac{-\xi_n^2}{2}, \frac{1-\xi_n^2}{2}\end{matrix}\right] \end{aligned} \tag{21}$$

4.2 Equal Gain Combining

An FSO system with EGC diversity consists of N number of photo detectors in the receiver. The N photo detector currents are combined and sent to the demodulator. The electrical SNR of the FSO system with EGC can be described as

$$SNR_{EGC} = \frac{\gamma^2}{2N^2\sigma_n^2}\left(\sum_{n=1}^{N} h_n\right)^2 \tag{22}$$

The probability of conditional BER can be defined as

$$P_{ec,EGC}(\boldsymbol{h}) = Q\left(\sqrt{SNR_{EGC}}\right) = 0.5 \times \operatorname{erfc}\left(\frac{\gamma}{2N\sigma_n}\sum_{n=1}^{N} h_n\right) \tag{23}$$

The average BER of SIMO–FSO system with EGC diversity can be expressed from Eq. (11) as

$$P_{e,EGC} = 0.5 \times \int_0^{\infty} \text{erfc}\left(\frac{\gamma}{2N\sigma_n}\sum_{n=1}^{N} h_n\right) f_{\boldsymbol{h}}(\boldsymbol{h})\, d\boldsymbol{h} \tag{24}$$

The above integral can be evaluated by expressing the complementary error function as Meijer G function [29, Eq. (8.4.14.2)] and using [31, Eq. (21)]. The proof is available in Appendix 3.

$$P_{e,EGC} = \prod_{n=1}^{N} \frac{2^{\alpha_n+\beta_n-4}\xi_n^2}{\sqrt{\pi^3}\Gamma(\alpha_n)\Gamma(\beta_n)} G_{7,4}^{2,6}\left[\frac{4\gamma^2 A_0^2 h_l^2}{N^2\sigma_n^2\alpha^2\beta_n^2}\middle|\begin{matrix}\frac{1-\xi_n^2}{2}, \frac{2-\xi_n^2}{2}, \frac{1-\alpha_n}{2}, \frac{2-\alpha_n}{2}, \frac{1-\beta_n}{2}, \frac{2-\beta_n}{2}, 1 \\ 0, \frac{1}{2}, \frac{-\xi_n^2}{2}, \frac{-\xi_n^{2+1}}{2}\end{matrix}\right] \tag{25}$$

4.3 Selection Combining

This is the simplest and least complex receiver diversity technique among the SIMO receiver combining schemes. In this technique, the aperture receiving maximum SNR is considered. The other apertures having less SNR are discarded. The selection is made according to [25]

$$h_{SC} = \max(h_1, h_2, \ldots . h_n) \tag{26}$$

The electrical SNR of the FSO system with SC can be described as

$$SNR_{SC} = \frac{(\gamma h_{SC})^2}{2N\sigma_n^2} \tag{27}$$

The probability of conditional BER can be defined as

$$P_{ec,SC}(h_{SC}) = Q\left(\sqrt{SNR_{SC}}\right) = 0.5 \times \text{erfc}\left(\frac{\gamma h_{SC}}{2\sqrt{N}\sigma_n}\right) \tag{28}$$

The average BER of SIMO–FSO system with EGC diversity can be expressed as

$$P_{e,SC} = 0.5 \times \int_0^{\infty} \text{erfc}\left(\frac{\gamma h_{SC}}{2\sqrt{N}\sigma_n}\right) f_h(h_{SC})\, dh_{SC} \tag{29}$$

The PDF of h_{SC} can be expressed as

$$f_{h_{SC}}(h_{SC}) = \frac{d}{dh_{SC}} F_{h_{SC}}(h_{SC}) = \sum_{i=1}^{N}\prod_{j=1, j\neq i}^{N} f_{h_i}(h_{SC})\, F_{h_j}(h_{SC}) \tag{30}$$

By applying Eq. (30) in (29), the average BER can be calculated as

$$P_{e,SC} = 0.5 \times \sum_{i=1}^{N}\prod_{j=1, j\neq i}^{N} \int_0^{\infty} \text{erfc}\left(\frac{\gamma h_{SC}}{2\sqrt{N}\sigma_n}\right) f_{h_i}(h_{SC})\, F_{h_j}(h_{SC})\, dh_{SC} \tag{31}$$

Where the cumulative distribution function (CDF), $F_h(h_{SC})$ can be evaluated as [7]

$$F_{h_{SC}}(h_{SC}) = \frac{\xi^2}{\Gamma(\alpha)\Gamma(\beta)} G_{2,4}^{3,1}\left[\frac{\alpha\beta}{A_0 h_l} h_{SC}\middle|\begin{matrix}1, \xi^2+1 \\ \xi^2, \alpha, \beta, 0\end{matrix}\right] \tag{32}$$

The integral in Eq. (31) can be evaluated by the Gaussian quadrature rule (GQR).

5 Numerical Results and Discussions

In this section, certain numerical results based on the analytical expressions derived in Sects. 3 and 4 are presented. For the numerical evaluations, the following FSO system parameters are considered.

Noise standard deviation $\sigma_n = 10^{-7}$A/Hz, photo detector responsivity $\gamma = 0.5$A/W, beam radius $w_L \cong 2.5$ m at 1 km distance and jitter standard deviation $\sigma_s \cong 30$ cm.

The simulation and analytical results of the BPSK–SIM based SISO and SIMO–FSO system are plotted for three apertures at the receiver ($N = 3$) and for $\alpha = 4, 1$ and $\beta = 1$ in Fig. 1. It is clearly depicted that the average BER performance of the SIMO system is improved, compared to the SISO–FSO system. From Fig. 1, it can be noticed that the higher values of α and β (strong turbulence) gives a better performance compared with lower values of α and β (very strong turbulence). Among the various diversity techniques considered, a better BER performance can be obtained for SC with $\alpha = 4$ and $\beta = 1$. Also Fig. 1 demonstrates that the average BER is improved along with responsivity of the photo detector. The preferred sensitivity of the photodetetor is around 0.4–0.6 A/W.

In Figs. 2 and 3, the two different values of $\alpha = 4, 1$ and $\beta = 1$ represent strong and very strong turbulence respectively. It can be seen from Figs. 1, 2, 3 and 4, by increasing the number of receiver apertures, significant average BER performance can be improved with respect to responsivity of the photo detector. A better BER performance I achieved through multiple receiver apertures.

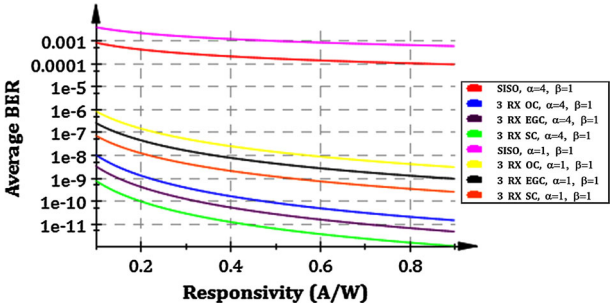

Fig. 1 BER against responsivity for SISO and SIMO–FSO systems with $\alpha = 4$, $\beta = 1$ and $\alpha = 1$, $\beta = 1$

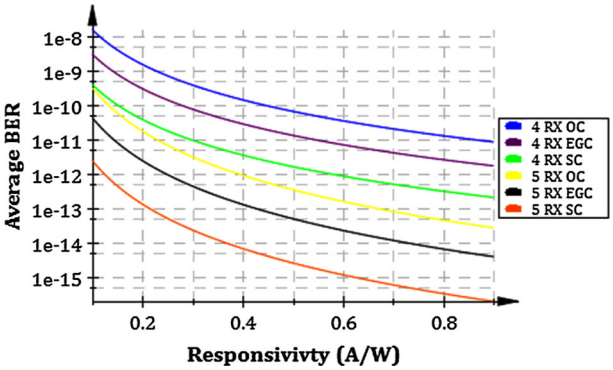

Fig. 2 BER against responsivity for SIMO–FSO system with $\alpha = 4$, $\beta = 1$ and $N = 4, 5$

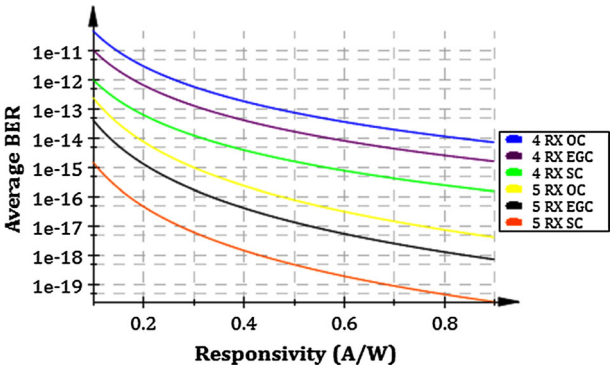

Fig. 3 BER against responsivity for SIMO–FSO system with $\alpha = 1$, $\beta = 1$ and $N = 4, 5$

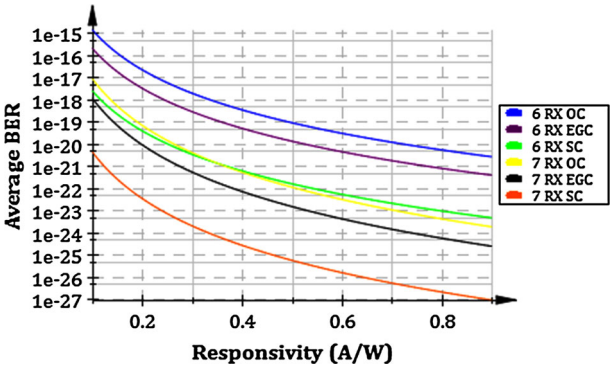

Fig. 4 BER against responsivity for SIMO–FSO system with $\alpha = 4$, $\beta = 1$ and $N = 6, 7$

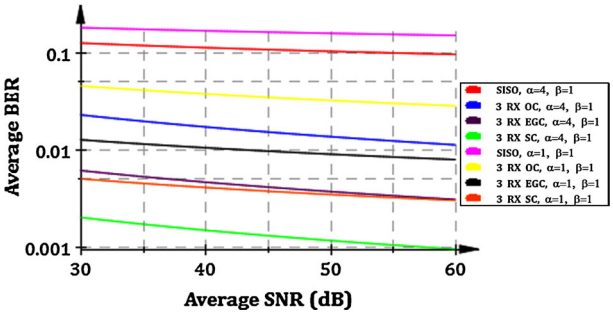

Fig. 5 BER against SNR for SISO and SIMO–FSO systems with $\alpha = 4$, $\beta = 1$ and $\alpha = 1$, $\beta = 1$

Figure 5 shows that a better average BER performance is achieved by using the SIMO system in terms of average SNR. It can be noticed that the average BER performance can be improved, by increasing the number of receive apertures. From the Figs. 5, 6, 7, 8 and 9, it is inferred that the FSO system with SC diversity ($N = 7, \alpha = 4, \beta = 1$) gives a better error rate performance of 10^{-6} for $SNR = 40\,\text{dB}$.

The 3D plots shown in Fig. 10 depicts the trade-off between the average BER against the effective number of large scale (α) and small scale (β) turbulent eddies for SISO, SIMO

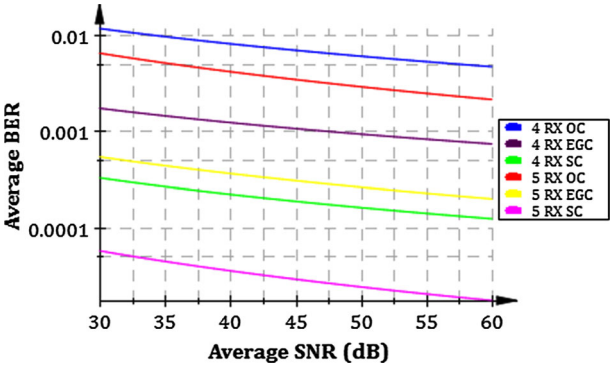

Fig. 6 BER against SNR for SIMO–FSO system with $\alpha = 4$, $\beta = 1$ and $N = 4, 5$

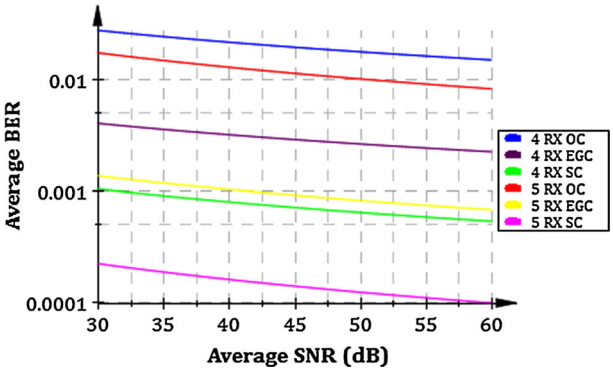

Fig. 7 BER against SNR for SIMO–FSO system with $\alpha = 1$, $\beta = 1$ and $N = 4, 5$

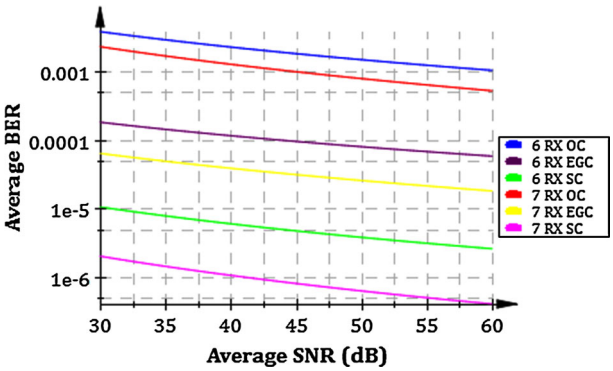

Fig. 8 BER against SNR for SIMO–FSO systems with $\alpha = 4$, $\beta = 1$ and $N = 6, 7$

with OC, EGC and SC combining schemes respectively. The 3D graphs are plotted only for the values of $\alpha = \beta = 4$. From Fig. 10, it is inferred that a better error rate performances are achieved for large values of $\alpha = \beta = 4$. The BER values are $0.15{,}5 \times 10^{-3}$, 10^{-4} and 10^{-5} for SISO, SIMO with OC, EGC and SC diversity using seven receiver apertures respectively ($N = 7$). From the aforementioned values, SIMO with diversity techniques providing a better BER performance compared with SISO system.

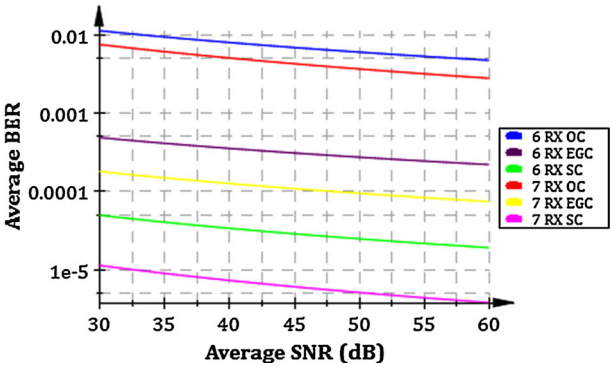

Fig. 9 BER against SNR for SIMO–FSO system with $\alpha = 1$, $\beta = 1$ and $N = 6, 7$

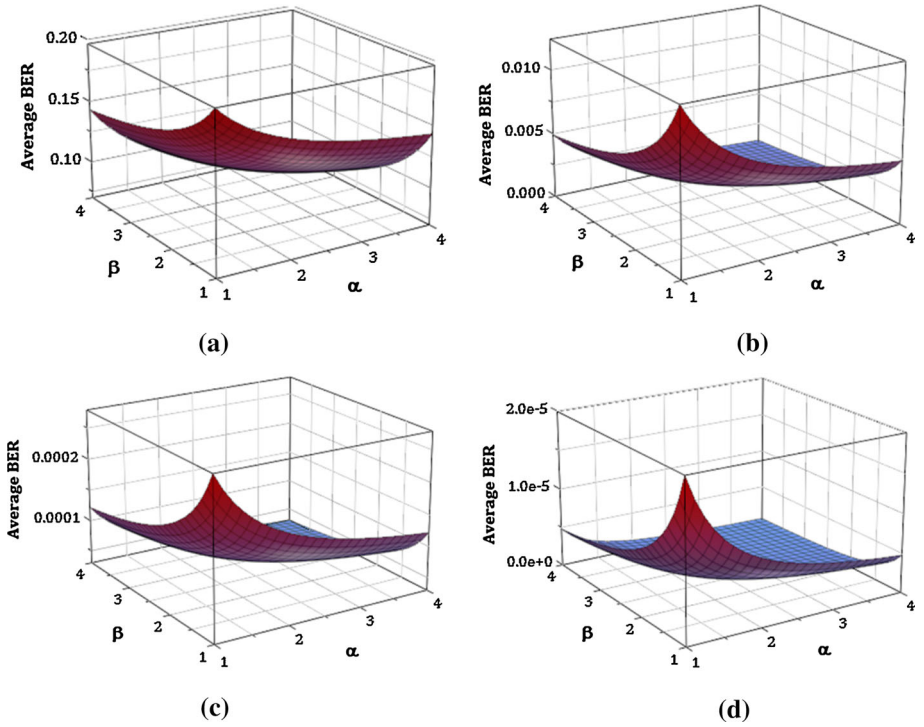

Fig. 10 3D plot for BER variation with respect to α and β for **a** SISO, **b** OC, **c** EGC, **d** SC

6 Conclusions

The novel exact closed-form expressions for the average BER of BPSK-SIM based SISO and SIMO–FSO systems over a strong atmospheric channel with pointing errors are derived. It is observed that SC provides the best BER performance compared to other considered combining schemes. It is also shown that a large number of receiving apertures offer a better BER performance. In addition, this work presents the simulation of BER performances of

SIMO with a maximum of seven receiver apertures. A better BER performance is achieved by using SIMO with SC combining is 10^{-5} at $SNR = 30\,\text{dB}$.

Appendix 1: Proof of BER of SISO [Eq. (13)]

The probability of average BER expressed by Eq. (12) is reproduced

$$P_{e,SISO} = \frac{\alpha\beta\xi^2}{A_0 h_l \Gamma(\alpha)\Gamma(\beta)} \times \int_0^\infty 0.5\,\text{erfc}\left(\frac{h\gamma}{2\sigma_n}\right) \times G_{1,3}^{3,0}\left[\frac{\alpha\beta h}{A_0 h_l}\Big|_{-1+\xi^2,\alpha-1,\beta-1}^{\xi^2}\right] dh \tag{33}$$

The complementary error function erfc $(\cdot)$ can be expressed as Meijer G function using Eq. (34). Using this identity, Eq. (33) reduces to (35)

$$\text{erfc}\left(\sqrt{x}\right) = \frac{1}{\sqrt{\pi}} G_{1,2}^{2,0}\left[x|_{0,1/2}^{1}\right] \tag{34}$$

$$P_{e,SISO} = \frac{\alpha\beta\xi^2}{A_0 h_l \Gamma(\alpha)\Gamma(\beta)} \times \int_0^\infty \frac{1}{2\sqrt{\pi}} G_{1,2}^{2,0}\left[\frac{\gamma^2 h^2}{4\sigma_n^2}\Big|_{0,1/2}^{1}\right] \times G_{1,3}^{3,0}\left[\frac{\alpha\beta h}{A_0 h_l}\Big|_{-1+\xi^2,\alpha-1,\beta-1}^{\xi^2}\right] dh \tag{35}$$

By using [31, Eq. (21)] in (35), Eq. (13) can be obtained.

Appendix 2: Proof of BER of SIMO with OC [Eq. (20)]

The strong atmospheric channel model (Eq. (9)) and the average BER of SIMO–FSO with OC (Eq. (19)) are reproduced respectively

$$f_{h_n}(h_n) = \frac{\alpha_n\beta_n\xi_n^2}{A_{0_n} h_{l_n} \Gamma(\alpha_n)\Gamma(\beta_n)} G_{1,3}^{3,0}\left[\frac{\alpha_n\beta_n h_n}{A_{0_n} h_{l_n}}\Big|_{-1+\xi_n^2,\alpha_n-1,\beta_n-1}^{\xi_n^2}\right] \tag{36}$$

$$P_{e,OC} \approx \frac{1}{12}\prod_{n=1}^{N}\int_0^\infty f_{h_n}(h_n)\, e^{-\left(\frac{\gamma^2 h_n^2}{4N\sigma_n^2}\right)} dh_n + \frac{1}{4}\prod_{n=1}^{N}\int_0^\infty f_{h_n}(h_n)\, e^{-\left(\frac{\gamma^2 h_n^2}{3N\sigma_n^2}\right)} dh_n \tag{37}$$

By applying Eq. (36) in (37)

$$P_{e,OC} \approx \frac{1}{12}\prod_{n=1}^{N}\int_0^\infty \frac{\alpha_n\beta_n\xi_n^2}{A_{0_n} h_{l_n} \Gamma(\alpha_n)\Gamma(\beta_n)} G_{1,3}^{3,0}\left[\frac{\alpha_n\beta_n h_n}{A_{0_n} h_{l_n}}\Big|_{-1+\xi_n^2,\alpha_n-1,\beta_n-1}^{\xi_n^2}\right] e^{-\left(\frac{\gamma^2 h_n^2}{4N\sigma_n^2}\right)} dh_n + \frac{1}{4}\prod_{n=1}^{N}\int_0^\infty \frac{\alpha_n\beta_n\xi_n^2}{A_{0_n} h_{l_n} \Gamma(\alpha_n)\Gamma(\beta_n)} G_{1,3}^{3,0}\left[\frac{\alpha_n\beta_n h_n}{A_{0_n} h_{l_n}}\Big|_{-1+\xi_n^2,\alpha_n-1,\beta_n-1}^{\xi_n^2}\right] e^{-\left(\frac{\gamma^2 h_n^2}{3N\sigma_n^2}\right)} dh_n \tag{38}$$

An exponential function exp (·) can be expressed as Meijer G function using Eq. (39). Using this identity, Eq. (38) can be simplified to (40).

$$\exp(-x) = G_{0,1}^{1,0}\left[x\middle|_{0}^{\cdot}\right] \tag{39}$$

$$\begin{aligned} P_{e,OC} \approx & \frac{1}{12}\prod_{n=1}^{N}\frac{\alpha_n\beta_n\xi_n^2}{A_{0_n}h_{l_n}\Gamma(\alpha_n)\Gamma(\beta_n)}\int_0^{\infty} G_{1,3}^{3,0}\left[\frac{\alpha_n\beta_n h_n}{A_{0_n}h_{l_n}}\middle|_{-1+\xi_n^2,\alpha_n-1,\beta_n-1}^{\xi_n^2}\right] \\ & G_{0,1}^{1,0}\left[\frac{\gamma^2 h_n^2}{4N\sigma_n^2}\middle|_{0}^{-}\right]dh_n \\ & + \frac{1}{4}\prod_{n=1}^{N}\frac{\alpha_n\beta_n\xi_n^2}{A_{0_n}h_{l_n}\Gamma(\alpha_n)\Gamma(\beta_n)}\int_0^{\infty} G_{1,3}^{3,0}\left[\frac{\alpha_n\beta_n h_n}{A_{0_n}h_{l_n}}\middle|_{-1+\xi_n^2,\alpha_n-1,\beta_n-1}^{\xi_n^2}\right] \\ & G_{0,1}^{1,0}\left[\frac{\gamma^2 h_n^2}{3N\sigma_n^2}\middle|_{0}^{-}\right]dh_n \end{aligned} \tag{40}$$

By using [31, Eq. (21)] in (40), Eq. (20) can be obtained.

Appendix 3: Proof of BER with EGC [Eq. (25)]

The average BER of SIMO–FSO with EGC (Eq. (24)) is reproduced

$$P_{e,EGC} = 0.5 \times \int_0^{\infty} \operatorname{erfc}\left(\frac{\gamma}{2N\sigma_n}\sum_{n=1}^{N} h_n\right) f_h(h)\,dh \tag{41}$$

By applying Eq. (36) in (41)

$$\begin{aligned} P_{e,EGC} = & 0.5 \times \frac{\alpha_n\beta_n\xi_n^2}{A_{0_n}h_{l_n}\Gamma(\alpha_n)\Gamma(\beta_n)}\int_0^{\infty}\operatorname{erfc}\left(\frac{\gamma}{2N\sigma_n}\sum_{n=1}^{N} h_n\right) \\ & G_{1,3}^{3,0}\left[\frac{\alpha_n\beta_n h_n}{A_{0_n}h_{l_n}}\middle|_{-1+\xi_n^2,\alpha_n-1,\beta_n-1}^{\xi_n^2}\right]dh_n \end{aligned} \tag{42}$$

The complementary error function erfc (·) can be expressed as Meijer G function using Eq. (34). Using this identity, Eq. (42) reduces to (43).

$$\begin{aligned} P_{e,EGC} = & \frac{\alpha_n\beta_n\xi_n^2}{2\sqrt{\pi}A_{0_n}h_{l_n}\Gamma(\alpha_n)\Gamma(\beta_n)}\prod_{n=1}^{N}\int_0^{\infty} G_{1,3}^{3,0}\left[\frac{\alpha_n\beta_n h_n}{A_{0_n}h_{l_n}}\middle|_{-1+\xi_n^2,\alpha_n-1,\beta_n-1}^{\xi_n^2}\right] \\ & G_{1,2}^{2,0}\left[\frac{\gamma^2 h_n^2}{4N\sigma_n^2}\middle|_{0,0.5}^{1}\right]dh_n \end{aligned} \tag{43}$$

By using [31, Eq. (21)] in (43), Eq. (25) can be obtained.

References

1. Kedar, D., & Arnon, S. (2004). Urban optical wireless communication networks: The main challenges and possible solutions. *IEEE Communications Magazine*, *42*(5), 2–7.

2. Gappmair, W., Hranilovic, S., & Leitgeb, E. (2010). Performance of PPM on terrestrial FSO links with turbulence and pointing errors. *IEEE Communications Letters*, *14*(5), 468–470.
3. Li, J., Liu, J. Q., & Taylor, D. P. (2007). Optical communication using subcarrier PSK intensity modulation through atmospheric turbulence channels. *IEEE Transactions on Communications*, *55*(8), 1598–1606.
4. Popoola, W. O., & Ghassemlooy, Z. (2009). BPSK subcarrier intensity modulated free-space optical communications in atmospheric turbulence. *Journal of Lightwave Technology*, *27*(8), 967–973.
5. Nistazakis, H. E., Karagianni, E. A., Tsigopoulos, A. D., Fafalios, M. E., & Tombras, G. S. (2009). Average capacity of optical wireless communication systems over atmospheric turbulence channels. *Journal of Lightwave Technology*, *27*(8), 974–979.
6. Farid, A. A., & Hranilovic, S. (2007). Outage capacity optimization for free-space optical links with pointing errors. *Journal of Lightwave technology*, *25*(7), 1702–1710.
7. Sandalidis, H. G., Tsiftsis, T. A., & Karagiannidis, G. K. (2009). Optical wireless communications with heterodyne detection over turbulence channels with pointing errors. *Journal of Lightwave Technology*, *27*(20), 4440–4445.
8. Sandalidis, H. G., Tsiftsis, T. A., Karagiannidis, G. K., & Uysal, M. (2008). BER performance of FSO links over strong atmospheric turbulence channels with pointing errors. *IEEE Communications Letters*, *12*(1), 44–46.
9. Zhu, X., & Kahn, J. M. (2002). Free-space optical communication through atmospheric turbulence channels. *IEEE Transactions on Communications*, *50*(8), 1293–1300.
10. Uysal, M., Navidpour, S. M., & Li, J. (2004). Error rate performance of coded free-space optical links over strong turbulence channels. *IEEE Communications Letters*, *8*(10), 635–637.
11. Zhu, X., & Kahn, J. M. (2003). Performance bounds for coded free-space optical communications through atmospheric turbulence channels. *IEEE Transactions on Communications*, *51*(8), 1233–1239.
12. Kiasaleh, K. (2005). Performance of APD-based, PPM free-space optical communication systems in atmospheric turbulence. *IEEE Transactions on Communications*, *53*(9), 1455–1461.
13. Kiasaleh, K. (2006). Performance of coherent DPSK free-space optical communication systems in K-distributed turbulence. *IEEE Transactions on Communications*, *54*(4), 604–607.
14. Tang, X., Ghassemlooy, Z., Rajbhandari, S., Popoola, W. O., & Lee, C. G. (2011). Coherent optical binary polarisation shift keying heterodyne system in the free-space optical turbulence channel. *IET Microwaves, Antennas & Propagation*, *5*(9), 1031–1038.
15. Betti, S., De Marchis, G., & Iannone, E. (1992). Polarization modulated direct detection optical transmission systems. *Journal of Lightwave Technology*, *10*(12), 1985–1997.
16. Huang, W., Takayanagi, J., Sakanaka, T., & Nakagawa, M. (1993). Atmospheric optical communication system using subcarrier PSK modulation. *IEICE Transactions on Communications*, *76*(9), 1169–1177.
17. Bayaki, E., Schober, R., & Mallik, R. K. (2009). Performance analysis of MIMO free-space optical systems in gamma-gamma fading. *IEEE Transactions on Communications*, *57*(11), 3415–3424.
18. Safari, M., & Hranilovic, S. (2013). Diversity and multiplexing for near-field atmospheric optical communication. *IEEE Transactions on Communications*, *61*(5), 1988–1997.
19. Lee, E. J., & Chan, V. W. (2004). Part 1: Optical communication over the clear turbulent atmospheric channel using diversity. *IEEE Journal on Selected Areas in Communications*, *22*(9), 1896–1906.
20. Yazgan, A., & Cavdar, I. H. (2013). The tradeoff between bit error rate and optical link distance using laser phase noise fixing process in coherent optical OFDM systems. *Wireless Personal Communications*, *68*(3), 907–919.
21. Hajjar, H., Fracasso, B., & Leroux, D. (2013). Fiber-distributed indoor high bitrate optical wireless system. *Wireless Personal Communications*, *72*, 1771–1782.
22. Barabino, N., & Rodríguez, B. (2013). Performance evaluation of FSO and MMW for the Uruguayan weather conditions. *Wireless Personal Communications, 73*(3), 1077–1088.
23. Rashed, A. N. Z., & Sharshar, H. A. (2013). Performance evaluation of short range underwater optical wireless communications for different ocean water types. *Wireless Personal Communications, 72*(1), 693–708.
24. Bhatnagar, M. (2013). Differential decoding of SIM DPSK over FSO MIMO links. *IEEE Communication Letters*, *17*(1), 1–4.
25. Tsiftsis, T. A., Sandalidis, H. G., Karagiannidis, G. K., & Uysal, M. (2009). Optical wireless links with spatial diversity over strong atmospheric turbulence channels. *IEEE Transactions on Wireless Communications*, *8*(2), 951–957.
26. Andrews, L. C., & Philips, R. L. (2005). *Laser beam propagation through random media* (2nd ed.). Washington, USA: SPIE Publications.
27. Lee, I. E., Ghassemlooy, Z., Ng, W. P. & Uysal, M. (2012). Performance analysis of free space optical links over turbulence and misalignment induced fading channels. In *Proceedings of the 8th IEEE/IET*

international symposium on communication systems, networks and digital signal processing (CSNDSP), pp. 1–6.
28. Prabu, K., Cheepalli, S., & Kumar, D. S. (2014). Analysis of PolSK based FSO system using wavelength and time diversity over strong atmospheric turbulence with pointing errors. *Optics Communications*, *324*, 318–323.
29. Prudnikov, A. P., Brychkov, Y. A., & Marichev, O. I. (1986). *Integral and series, vol. 3: More special functions*. Amsterdam: Gordon and Breach Science Publishers.
30. Prabu, K., Bose, S., & Sriram Kumar, D. (2013). BPSK based subcarrier intensity modulated free space optical system in combined strong atmospheric turbulence. *Optics Communications*, *305*, 185–189.
31. Adamchik, V. S., & Marichev, O. I. (1990). The algorithm for calculating integrals of hyper geometric type functions and its realization in REDUCE system. In *Proceedings of international conference on symbolic and algebraic computation* Tokyo, Japan, pp. 212–224.
32. Chiani, M., Dardari, D., & Simon, M. K. (2003). New exponential bounds and approximations for the computation of error probability in fading channels. *IEEE Transactions on Wireless Communications*, *2*(4), 840–845.

K. Prabu received his Bachelor in Engineering Degree in Electronics and Communication Engineering and the Master of Engineering Degree in Communication and Networking from Anna University, Chennai, India, in 2007 and 2010 respectively. Currently he is pursuing his Ph.D. in Free Space Optical Communication in the Department of Electronics and Communication Engineering, National Institute of Technology (NIT), Tiruchirappalli, India. He is a recipient of Technical Education Quality Improvement Programme (TEQIP) Scholarship (2012–2015) for his Ph.D Program in the Department of Electronics and Communication Engineering, National Institute of Technology (NIT), Tiruchirappalli, India. His research interests include free-space optical (FSO) communications, wireless communications, visible light communication (VLC), multiple-input multiple-output (MIMO) systems, and radio over fiber (RoF) technology and radio over free space optical (RoFSO) communications.

D. Sriram Kumar received his Bachelor in Engineering Degree in Electronics and Communication Engineering from Madurai Kamaraj University, India in 1991 and the Master of Engineering Degree in Microwave and Optical Engineering, from A.C. College of Engineering and Technology, Karaikudi, India, in 1994. He received the Ph.D. degree in Electronics and Communication Engineering from the Bharathidasan University, India, in 2009. He is currently working as an Associate Professor in the Department of Electronics and Communication Engineering, National Institute of Technology (NIT), Tiruchirappalli, India. His current research interests include Optical Networks, Smart Antennas, Optical Communications, and Microwave integrated circuits.